

BAND GAP ENGINEERING FOR IMPROVED PHOTOCATALYTIC PERFORMANCE OF CuS/TiO₂ COMPOSITES UNDER SOLAR LIGHT IRRADIATION

M. Hassan Farooq^{1,2*}, I. Aslam³, Ahmad Shuaib², H. Sadia Anam⁴, M. Rizwan⁵, and Qudisia Kanwal⁶

¹Laboratory of Eco-Materials and Sustainable Technology, The Xinjiang Technical Institute of Physics and Chemistry, Chinese Academy of Sciences, Urumqi, Xinjiang 830011, P. R. China

²Basic Sciences and Humanities Department, University of Engineering and Technology, KSK Campus, Lahore, Pakistan

³Department of Basic Sciences and Humanities, University of Engineering and Technology, NWL Campus, Lahore, Pakistan

⁴Department of Chemistry, University of Lahore, Pakistan

⁵Department of Physics, University of Gujrat, Gujrat, Pakistan

⁶Department of Physics, University of Gujrat, Gujrat, Pakistan

(Received May 20, 2019; Revised July 1, 2019; Accepted July 21, 2019)

ABSTRACT. Nanoparticles of CuS, TiO₂ and CuS/TiO₂ composites were prepared by template free hydrothermal method. Prepared nanoparticles were characterized by X-ray diffraction (XRD) and electron dispersive X-ray spectroscopy to confirm the formation of nanoparticles. Field emission scanning electron microscopy (FESEM) was applied to investigate the morphology and particle size of the nanoparticles which were measured in the range of 30–40 nm. Photocatalytic performance of CuS, TiO₂ and CuS/TiO₂ were measured by degradation of methyl orange (MO) under solar light irradiation. Coupling of n-type TiO₂ (3.2 eV) with p-type CuS (1.9 eV) showed efficient degradation of the contaminants under the solar light irradiation. Photocatalytic performance of CuS/TiO₂ composite improves 1.4 times than CuS for the degradation of methyl orange (MO) under solar light irradiation.

KEY WORDS: CuS/TiO₂ composites, Photocatalytic performance, Hydrothermal growth, Solar light, Irradiation

INTRODUCTION

TiO₂ is widely used as a photocatalyst due low toxic, highly stable and of being low cost material. For the performance of photocatalytic reaction, TiO₂ have to interact with the photons of light having energy equal or greater than the band gap of TiO₂. Irradiation of each photon causes to excite the electron from valance band to the conduction band leaving behind the hole in valance band and one electron in the conduction band. For the best performance of TiO₂, two reactions occurred simultaneously, oxidation reaction of absorbed H₂O by the photogenerated hole and secondly reduction of oxygen molecule absorbed in the solution by photogenerated electron. Both oxidation and reduction reactions provide hydroxyl and superoxide radicals anion, respectively [1].

These charge carriers can transfer Ti⁺⁴ to Ti⁺³ and O⁻ defects. Electron-hole can recombine and dissipate the energy. The most effective way for photocatalyst is that charge carriers appear on the surface of catalyst and start redox reaction [2]. Holes at the valance band oxidize the absorbed water molecules and produce hydroxyl radicals which are more active. These hydroxyl radicals oxidize the organic species and produce mineral salts, CO₂ and H₂O [3]. Electron in the conduction band reduces the molecular oxygen absorbed in the solution to super oxide radical

*Corresponding author. mhfarooq@uet.edu.pk

This work is licensed under the Creative Commons Attribution 4.0 International License

anion ($O_2^{\bullet-}$) which further act with H^+ to give hydroperoxyl radical ($\bullet OOH$). This reactive oxygen further interacts with the organic pollutants to oxidize the molecules and degrade the pollutants.

Electron-hole pairs recombination is a main challenge for the limitation of photocatalytic reactions. For recombination, electron from the conduction band reverts to the valance band without reacting with absorbed species or reducing oxygen molecule. This recombination of electron-hole pairs dissipates the energy. It has been reported that reduction of Ti^{+4} to Ti^{+3} by excited electron takes place only for 30 ps and ninety percent of these electrons recombine within 10 ns [4]. Retardation for electron-hole recombination can improve the photocatalytic performance. Separation of electron-hole recombination can be controlled by doping of ions [5-9], heterojunction coupling [10-13], such as coupling with naturally p-type semiconductors and nanosized structures. For example, TiO_2 in the form of Evonik (Degussa) P 25 has the combination of rutile (20%) and anatase (80%). As the potential level of rutile is more positive than anatase so it works as a sink for photogenerated electron and inhibits the recombination of electron-hole pairs, results in the improvement of photocatalytic performance of TiO_2 [14].

Titania has a band gap of 3.2 eV which is active under UV-light region. UV region is 4-5% of solar light [15] while 45% of solar light lies in the visible light region. Efforts have been made to extend the activity of TiO_2 in visible light region. Following steps have been made to make it active under visible light region, i.e. non metal doping, metal deposition, coupled semiconductors, and defect induced visible light active photocatalyst.

In order to enhance the solar efficiency and make TiO_2 photocatalytic under visible light region, non metal doping shows great promising achievement in this regard. Nitrogen doping is considered to be the most promising dopant [16]. Nitrogen is considered most suitable and stable dopant for the substitutional position of oxygen of being comparable in size with oxygen and small ionization energy.

Fluorine doping to TiO_2 does not make the material photoactive under visible light but it reduces the Ti^{+4} to Ti^{+3} due to the charge exchange between Ti^{+4} and F. This causes to increase the acidity of surface. Compensation of charge between Ti^{+4} and F⁻ results in the separation of charges and increase the photocatalytic activity. Insertion of F also transforms the anatase phase of TiO_2 to rutile phase. Titanium isopropoxide was modified by using trifluoroacetic acid during sol-gel process by Padmanbhan [17]. The proposed material showed more photocatalytic activity than Evonik (P25) and also retained the anatase phase up to 900 °C.

Carbon, phosphorous and sulfur doping to TiO_2 have also reported for their photoactive response under visible light region [18, 19]. Doping of non metals changes the lattice sites and produces the trap sites within the conduction and valance band. These sites results in the formation of new energy levels above the valance band or below the conduction band. These shallow levels result in the reduction of band gap [20-22] and increase the life time of photo excited electrons due to the trap sites.

Co-doping of cationic sulfur (S^{+6}) and anionic nitrogen is reported by simple sol-gel technique [23] for its photoactive performance under visible light region and retained for the anatase phase up to 800 °C. TiO_2 is modified in oxygen rich atmosphere by the decomposition of titania peroxide to make the material active under visible light region [24]. Increased oxygen causes to strengthen the Ti-O-Ti and upward shifting of VB maximum. Upward shifting of VB is responsible for its activity under visible light.

Deposition of metal ions V, Cr, Co and Fe [25-28] on the surface of TiO_2 increase the spectral response of material to visible light region and improve the photocatalytic performance. But the transition metals on the surface themselves provide the recombination sites for charge carriers which cause to increase the electron-hole recombination ratio. The transition metal deposition also has low stability.

Photocatalytic performance can also be improved by introducing the defects inside the material [29]. These defects can be introduced by thermal treatment of TiO_2 in vacuum which

induce oxygen vacancies and reduced Ti⁺⁴ to Ti⁺³ providing new energy levels inside the band gap of TiO₂ to make it active under visible light region. Nowadays, an interesting and powerful tailoring of new energy levels is done by hydrogenation of TiO₂ at high temperature. Annealing at high temperature in hydrogen atmosphere extract the oxygen atoms from the surface level and reduced Ti⁺⁴ to Ti⁺³ and make it active under visible light [30].

Semiconductor coupling is another interesting tool. Large band gap and electron-hole recombination ratio are the main hindrances for the visible light response and high photocatalytic performance. Coupling of TiO₂ with low energy band gap semiconductors and p-type semiconductors make the material active for visible light region and improved photocatalytic performance such as ZnO/TiO₂, Bi₂S₃/TiO₂ [31] and CdS/TiO₂ [32].

Titanium dioxide (TiO₂) due to its high binding energy of 458.6 meV at room temperature has achieved extensive attention of researchers. Practically performance of titanium dioxide as photocatalyst is very low due to several factor including limited quantum efficiency, slower photocatalysis rate and larger band gap. TiO₂ has large band gap of 3.2 eV which shows activation under UV light region. Only ultraviolet light with frequency shorter than 385 nm can be used for the activation of TiO₂ photocatalyst and is a major challenge. Noble metal loading is one of the techniques used for visible light activation of TiO₂. Noble metals such as silver, gold and platinum can trap electrons, thus photocatalytic properties are improved by enhancing holes electron separation by the development of Schottky barrier at the interface of semiconductor-noble metal interface. Though noble metal loading can improve visible light activity of photocatalyst but high cost of these metals limit the chances for industrial use. One of the promising techniques is combining this large band gap semiconductor with small band gap semiconductors, i.e. CdSe, CdS, PbS which can enhance the absorption range toward visible light. But unfortunately environmental effects of Cd and Pb are uncompromisable due to toxicity. One of the major candidates is CuS which is cost effective and environment friendly.

TiO₂ has band gap of 3.2 eV which is too large for visible light activation while band gap of CuS is 1.9 eV that is too short to inhibit efficient recombination of electron-hole pairs immediately after their formation. Composite of CuS/TiO₂ semiconductors is prepared to investigate the improved photocatalytic performance for visible light region. A junction is formed at interface between CuS p-type and TiO₂ n-type. Electron-hole pair production in CuS causes to disturb the equilibrium of p-n junction which results in the transfer of electron to conduction band of TiO₂ and holes to the valance band of CuS. Photocatalytic activity of CuS/TiO₂ increases due to better electron-hole separation. CuS/TiO₂ composites can serve as a visible light active photocatalyst because of low band gap (1.9 eV) of CuS. Photoactivity of TiO₂ and CuS checked separately and after formation of junction. It is checked that CuS/TiO₂ composites show better visible light activity rather than TiO₂ and CuS separately.

EXPERIMENTAL

Fabrication of CuS/TiO₂ composites

Fabrication of CuS, TiO₂, and CuS/TiO₂ composites is done by using template free hydrothermal method. Chemicals used for the fabrication of TiO₂, CuS and their composites are titanium tetra isopropoxide (TTIP) Ti[OCH(CH₃)₂]₄, Cu(NO₃)₂·2H₂O, Na₂S·9H₂O, reducing agent KOH and deionized (DI) water. All these chemicals were purchased from Sigma Aldrich up to 97% pure and were used for fabrication without further purification.

First of all nanoparticles of TiO₂ and CuS are prepared by template free hydrothermal method. 0.05 M solution of TTIP is prepared in deionized water and 10 mL 0.02 M solution of reducing agent KOH is mixed in the solution of 30 mL solution of 0.05 M TTIP which is stirred at 60 °C for 30 min to get homogeneous and clear solution of TTIP. After getting clear and homogeneous solution of TTIP, precursor is transferred to 60 mL Teflon autoclave of stainless

steel. Autoclave is heated at 180 °C for 24 hours in an oven. At room temperature, material is taken out of the autoclave and washed several times with ethanol and water to remove the impurities and organic contents from the synthesized material. Final washed product is dried at 80 °C for six hours in air atmosphere to remove all other impurities and contents.

15 mL of 0.05 molar of $\text{Cu}(\text{NO}_3)_2 \cdot 2\text{H}_2\text{O}$ and $\text{Na}_2\text{S} \cdot 9\text{H}_2\text{O}$ solutions were prepared separately and then mixed drop wise during stirring. 10 mL of 0.02 M reducing agent KOH solution was used and mixed drop wise. After that precursor is stirred for few minutes and transferred to the 60 mL Teflon autoclave of stainless steel which is heated at 180 °C for 24 hours to get nanoparticles of CuS. Obtained material was washed with ethanol and water to remove the impurities and organic contents. Material was dried at 80 °C for six hours in air atmosphere.

CuS/TiO₂ composites were prepared by mixing the both final solutions before the transfer to Teflon autoclave of stainless steel. The solution was stirred for few minutes and transferred to 100 mL Teflon autoclave of stainless steel which is heated at 180 °C for 24 hours. Obtained material was washed and annealed in air atmosphere at 80 °C for six hours.

Characterization

X-ray diffraction analysis with $\text{CuK}\alpha$ radiation ($\lambda = 0.154 \text{ nm}$) was applied to characterize the structure of prepared nanoparticles. Field emission scanning electron microscopy (FESEM) and energy dispersive X-ray spectroscopy (EDS) was applied to analyze the morphology and composition of the prepared nanoparticles. UV-Vis-NIR spectroscopy for absorption spectrum was applied at room temperature to measure the band gap of the nanoparticles.

Photocatalytic activity

Photocatalytic performance of CuS, TiO₂ and CuS/TiO₂ composite was checked by preparing the 20 mg/L solution of methyl orange (MO). 0.05 g of catalyst was used in 20 mL solution of 20 mg/L. Solution was kept under constant stirring in darkness for 30 min to get equilibrium among the solution and catalyst. After that solution was put under solar lamp and stirred continuously. For checking the degradation of the pollutants, samples were taken from the solution with the interval of 20 min.

RESULTS AND DISCUSSION

Crystalline nature and purity of CuS, TiO₂ and CuS/TiO₂ composites were characterized by XRD with $\text{CuK}\alpha$ radiation ($\lambda = 0.154 \text{ nm}$). It was found that peaks of CuS were in complete agreement with JCPD no. 06-0464 and no impurity peaks were observed and also confirmed the tetragonal crystalline structure. XRD pattern also confirmed the formation of TiO₂ and hexagonal structure of TiO₂. No impurity peaks were observed in the composites of CuS/TiO₂, all peaks were related to CuS and TiO₂.

Crystalline size of the particles was calculated by using the data of XRD peaks with the help of Debye-Scherrer formula: $D_c = K\lambda/\beta\text{Cos}\theta$, where K is constant and called shape factor with value of 0.9 for tetragonal structure, λ stands for the wavelength of X-rays which is 1.5406 Å for $\text{CuK}\alpha$, β stands for the full wave half maximum (FWHM) of the peak and θ indicates the Bragg's angle. Average crystalline size calculated for our synthesized material is 32 nm for CuS/TiO₂ composites. Figure 1 depicts the XRD pattern for CuS, TiO₂ and CuS/TiO₂ composite.

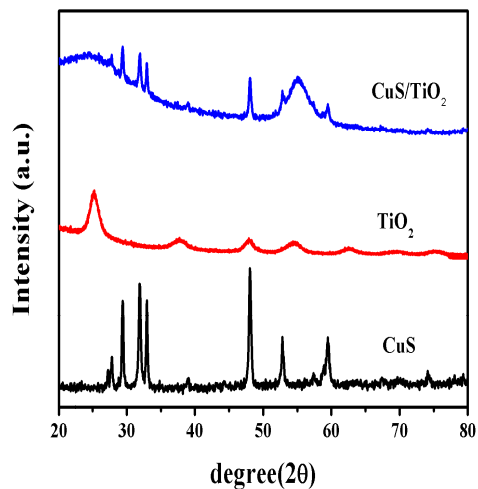


Figure 1. XRD pattern for CuS, TiO₂ and CuS/TiO₂ composites.

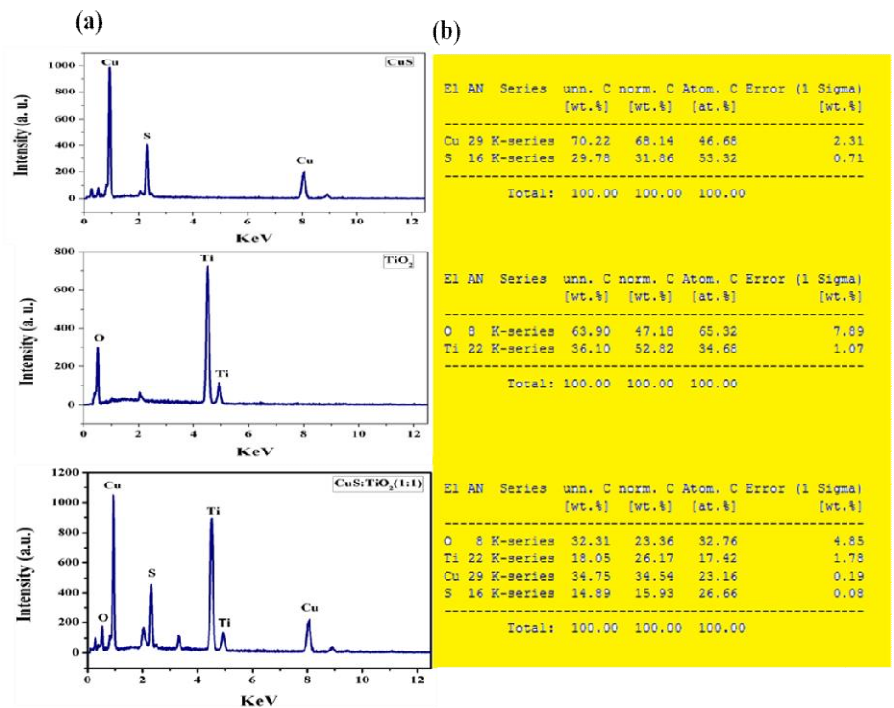


Figure 2. (a) EDS spectrum for CuS, TiO₂ and CuS/TiO₂ composites and (b) elemental composition data of O, Ti, Cu and S atoms.

Chemical decomposition of the materials was investigated by energy dispersive spectroscopy (EDS). EDS spectrum indicates that synthesized material has only the peaks of Ti, O, Cu and S which confirms that no impurity mixed in the synthesized material. EDS spectrum is shown in the Figure 2(a) along with the composition data of Ti, O, Cu and S atoms in Figure 2(b).

Morphology of the synthesized material is characterized by field emission scanning electron microscopy. Large surface area is required for the photocatalytic performance which is only possible with nanoparticle size growth. FESEM images for CuS, TiO₂, and CuS/TiO₂ composite is shown in Figure 3.

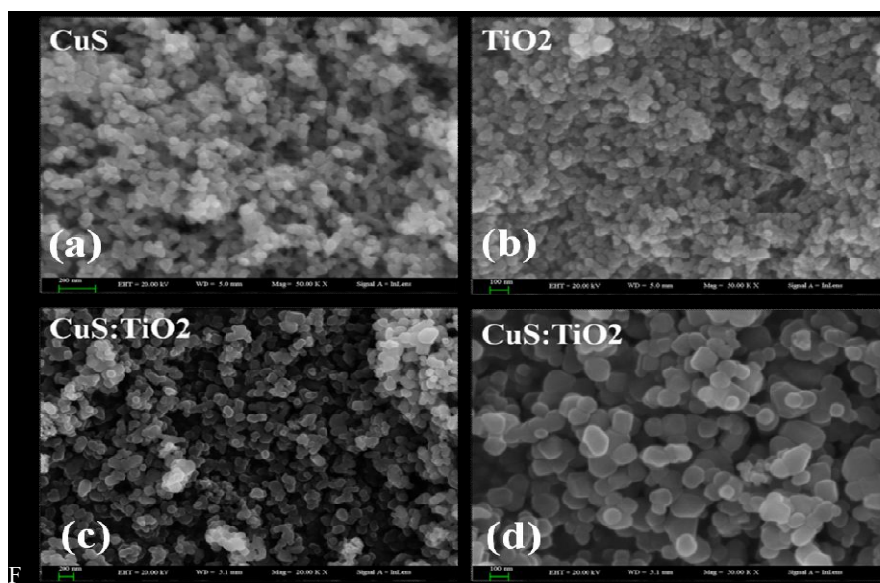


Figure 3. (a) FESEM images for CuS, (b) FESEM images for TiO₂, (c) and (d) FESEM images for CuS/TiO₂ composites.

All the particles are in the range of 30 nm to 40 nm size. Small size of these particles causes to produce large surface area to interact with photons of solar light which in return improved the photocatalytic performance of synthesized material.

Band gap is an important parameter to characterize the semiconductors to investigate their photoactive response under solar light irradiation. CuS is a p-type semiconductor having band gap of 1.9 eV while TiO₂ is an n-type semiconductor having band gap of 3.2 eV. Titania is a large band gap semiconductor active under UV region and works as a stable photocatalyst. CuS is small band gap material active under visible light region but it has high rate of electron-hole recombination. Composites of CuS/TiO₂ induce a pn-junction at the interface of both semiconductors results in lowering the electron-hole recombination rate. As band gap of CuS is 1.9 eV and has different NHE potential than TiO₂ which cause to reduce the band gap of resultant composite by introducing new Fermi level inside the band gap. Schematic diagram of CuS/TiO₂ composites is shown in Figure 4.

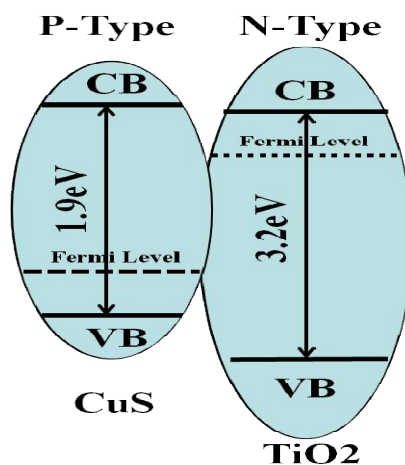


Figure 4. Schematic diagram for CuS and TiO₂ composite.

Band gap plays key role for photocatalytic performance of the material. Band gap can be calculated from UV-Visible spectroscopy. UV-Vis-spectroscopy is done in wavelength range from 480 nm to 800 nm which shows absorbance in visible light range. For calculation of band gap of the composite material CuS/TiO₂, we can make calculation by using the following relation: $(\alpha h\nu)^2 = B(h\nu - E_g)$.

Above relation is called Tauc relationship, α shows the absorption coefficient, E_g indicates the band gap while $h\nu$ stands for the photon energy of the incident light beam. Figure 5 indicates the UV-Vis spectrum in visible light range and calculated band gap of the synthesized material which is 1.89 eV.

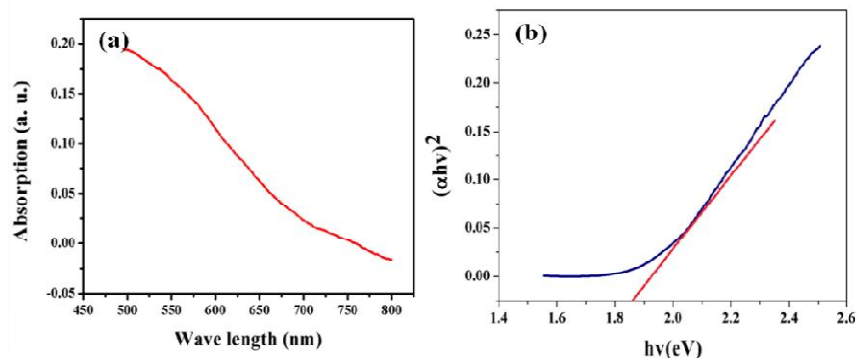


Figure 5. (a) UV-Vis spectrum under visible light and (b) band gap calculation for CuS/TiO₂ composite.

Figure 6 shows the photodegradation of the methyl orange under solar light irradiation. Figure 6(a), 6(b) and 6(c) shows the absorption peaks of UV-Vis spectroscopy of the collected samples of TiO₂, CuS, and CuS/TiO₂ respectively for the degradation of the pollutants under solar light irradiation while Figure 6(d) shows the comparison of the degradation of pollutants for CuS, TiO₂ and CuS/TiO₂ composites.

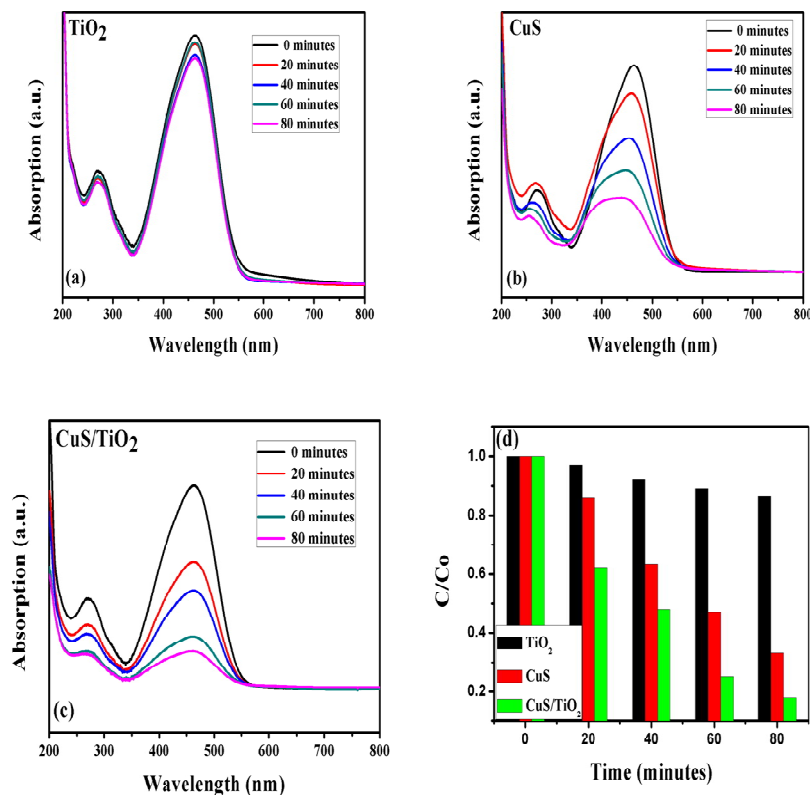
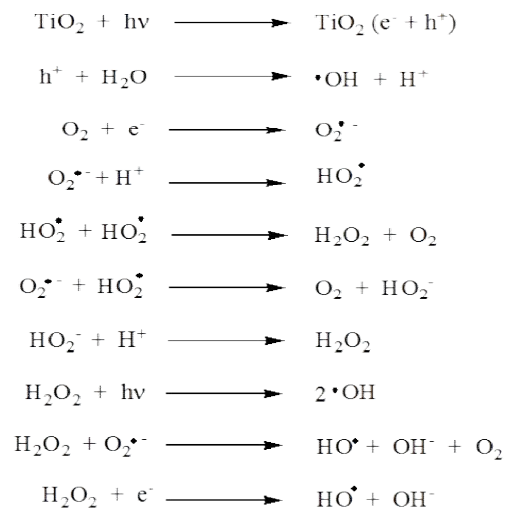


Figure 6. (a) Photodegradation of MO under solar light irradiation with TiO₂, (b) photodegradation of MO under solar light irradiation with CuS, (c) photodegradation of MO under solar light irradiation with CuS/TiO₂ and (d) comparison of photodegradation of MO under solar light irradiation with TiO₂, CuS and CuS/TiO₂.

From Figure 6 degradation of the pollutants can be observed TiO₂, CuS and CuS/TiO₂ composite. Titania degraded the MO upto 15% in solar light irradiation, CuS degraded the MO up to 60% in solar light irradiation while CuS/TiO₂ composite degraded the pollutant up to 80% in solar light irradiation.

CuS is low band gap semiconductor, in which electron-hole recombination rate is very high. When photon of light excites the electron from valance band to the conduction band, excited electron interacts with the absorbed oxygen molecule and reduces it to oxygen super oxide (O₂^{•-}) which is more active and react with the organic pollutants. Hole in the valance band interact with water molecule to transform the hydroxyl ion. A series of oxidation and reduction reactions occur due to the electron-hole pairs:



A major challenge for electron-hole pairs is the recombination without interaction with solvent and organic pollutants which is controlled by inducing depletion region at the interface of both semiconductors. Depletion region at the interface is formed due to the formation of pn-junction which is because of p-type nature of CuS and n-type nature of TiO₂. Depletion region at the interface inhibits the electron-hole recombination result in the improved photocatalytic performance.

CONCLUSION

CuS, TiO₂ and composites of CuS/TiO₂ were prepared by template free hydrothermal method. Synthesized nano particles were characterized by X-ray diffraction (XRD) by using CuK α radiations to confirm the crystal structure and formation of required material. Purity of the nanoparticles was investigated by energy dispersive spectroscopy (EDS) which confirms that no impurity peak exists in the material. Morphology and size of the synthesized nanoparticles were checked by field emission scanning electron microscopy (FESEM) which confirms the particle size upto 30-40 nm that provides the large surface area to interact with the incident photons of light to improve the photocatalytic performance. UV-Vis-spectroscopy calculated the band gap of semiconductor and observed the absorption in the visible light range. Composite of n-type TiO₂ with low band gap p-type CuS make the material photoactive under visible region. A depletion region is formed at the interface of both semiconductors which inhibits the electron-hole recombination and improved the photocatalytic performance of CuS/TiO₂ composite under solar light irradiation up to 80%.

ACKNOWLEDGEMENT

We are thankful to Higher Education Commission (HEC), Pakistan for providing financial support for this research work under National Research Project for Universities No. 8421/Punjab/NRPU/R&D/HEC/2017.

REFERENCES

1. Mills, A.; Hunte, S.L. An overview of semiconductor photocatalysis. *J. Photochem. Photobiol. A* **1997**, *108*, 1-35.
2. Cozzoli, P.D.; Comparelli, R.; Fanizza, E.; Curri, M.L.; Agostiano, A. Photocatalytic activity of organic-capped anatase TiO₂ anatase crystals in homogeneous organic solutions. *Mater. Sci. Technol. C* **2003**, *23*, 707-713.
3. Hoffman, A.J.; Carraway, E.R.; Hoffman, M.R. Photocatalytic production of H₂O₂ and organic peroxides on quantum sized semiconductor colloids. *Environ. Sci. Technol.* **1994**, *28*, 776-785.
4. Serpone, N.; Lawless, D.; Khairutdinov, R.; Pelizzetti, E. Size effects on the physical properties of colloidal anatase TiO₂ particles: Size quantization versus direct transition in this direct semiconductor. *J. Phys. Chem.* **1995**, *99*, 16646-16654.
5. Soria, J.; Conesa, J.C.; Augugliaro, V.; Palmisano, L.; Schiavello, M.; Sclafani, A. Dinitrogen to photoreduction to ammonia over titanium dioxide powders doped with ferric ions. *J. Phys. Chem.* **1991**, *95*, 274-282.
6. Yu, J.C.; Yu, J.; Ho, W.; Jiang, Z.; Zhang, L. Effect of F-doping on photocatalytic activity and microstructures of nanocrystalline TiO₂ powders. *Chem. Mater.* **2002**, *14*, 3808-3816.
7. Do, Y.R.; Lee, K.; Dwight, K.; Wold, W. The effect of WO₃ on the photocatalytic activity of TiO₂. *J. Solid State Chem.* **1994**, *108*, 198-201.
8. Engweiler, J.; Harf, J.; Baiker, A. WO_x/TiO₂ catalysts prepared by grafting of tungsten alkoxide: Morphological properties and catalytic behavior in the selective reduction of NO by NH₃. *J. Catal.* **1996**, *159*, 259-269.
9. Vinodgopal, K.; Kamat, P.V. Enhanced Rates of photocatalytic degradation of an azo dye using SnO₂/TiO₂ coupled semiconductor thin films. *Environ. Sci. Technol.* **1995**, *29*, 841-845.
10. Maira, A.J.; Yeung, K.L.; Lee, C.Y.; Yue, P.L.; Chan, C.K. Size effects on gas phase photo-oxidation of trichloroethylene using nano meter sized TiO₂ catalysts. *J. Catal.* **2000**, *192*, 185-196.
11. Aregahegn, Z.; Guesh, K.; Chandravanshi, B.S.; Perez, E. Application of chemometric methods to resolve intermediates formed during photocatalytic degradation of methyl orange and textile wastewater from Ethiopia. *Bull. Chem. Soc. Ethiop.* **2017**, *31*, 23-32.
12. Fujishima, A.; Zhang, X.; Tryk, D.A. TiO₂ photocatalysis and related surface phenomena. *Surface Sci. Rep.* **2008**, *63*, 515-582.
13. Mebrahtu C.; Tadesse A.M.; Goro, G.; Yohannes, T. Natural pigment sensitized solar cells based on ZnO -TiO₂-Fe₂O₃ nanocomposites in quasi-solid state electrolyte system. *Bull. Chem. Soc. Ethiop.* **2017**, *31*, 263-279.
14. Emeline, A.V.; Kuznetsov, V.N.; Rybchuk, V.K.; Serpone, N. Visible light active titania photocatalysts: The case of N-doped TiO₂, properties and some fundamental issues. *Int. J. Photoenergy* **2008**, *2008*, Article ID 258394.
15. Nunez M.; Forgan B.; Roy C. Estimating ultraviolet radiations at the earth's surface. *Int. J. Biometeorol.* **1994**, *38*, 5-17.
16. Serpone, N. Is the band gap of pristine TiO₂ narrowed by anion and cation doping of titanium dioxide of second - generation photocatalysts? *J. Phys. Chem. B* **2006**, *110*, 24287-24293.

17. Padmanabhan, S.C.; Pillai, S.C.; Colreavy, J.; Balakrishna, S.; McCormack, D.E.; Perova, T. S.; Gunko, Y.; Hinder, S.J.; Kelly J.M. A. simple sol-gel processing for the development of high temperature stable photoactive anatase titania. *Chem. Mater.* **2007**, *19*, 4474-4481.
18. Irie, H.; Watanabe, Y.; Hashimoto, K. Carbon doped anatase TiO₂ powders as visible light sensitive photocatalyst. *Chem. Lett.* **2003**, *32*, 772-773.
19. Sakthivei, S.; Kisch, H. Daylight photocatalysis by carbon-modified titanium dioxide. *Angew. Chem. Int. Ed.* **2003**, *42*, 4908-4911.
20. Nagabeni, K.; Hedge, M.S.; Ravishankar, N.; Subbana, G.N.; Madras, G. Synthesis and structure nanocrystalline TiO₂ with lower band gap showing high photocatalytic activity. *Langmuir* **2004**, *20*, 2900-2907.
21. Umebayashi, T.; Yamaki, T.; Itoh, H.; Asahi, K. Band gap narrowing of titanium dioxide by sulfur doping. *Appl. Phys. Lett.* **2002**, *81*, 454-456.
22. Kamal, D.B.; Klabunde, K.J. Synthesis, characterization and visible light activity of new nanoparticle photocatalysts based on silver, carbon and sulfur doped TiO₂. *J. Colloid Interface Sci.* **2007**, *311*, 514-522.
23. Periyat, P.; McCormack, D.E.; Hinder, S.J.; Pillai, S.C. One-pot synthesis of anionic (nitrogen) and cationic (sulfur) codoped high temperature stable, visible light active, anatase photocatalysts. *J. Phys. Chem. C* **2009**, *113*, 3246-3235.
24. Etacheri, V.; Seery, M.K.; Hinder, S.J.; Pillai, S.C. Oxygen rich titania: A dopant free, high temperature stable, and visible light active anatase photocatalyst. *Adv. Functional Mater.* **2011**, *21*, 3744-3752.
25. Klosek, S.; Raftery, D. Visible light driven V-doped TiO₂ photocatalyst and its photooxidation of ethanol. *J. Phys. Chem. B* **2001**, *105*, 2815-2819.
26. Borgarello, E.; Kiwi, J.; Gratzel, M.; Pelizzetti, E.; Visca, M. Visible light induced water cleavage in colloidal solutions of chromium doped titanium dioxide particles. *J. Am. Chem. Soc.* **1982**, *104*, 2996-3002.
27. Iwasaki, M.; Hara, M.; Kawada, H.; Tada, H.; Ito, S. Cobalt ion doped TiO₂ photocatalyst response to visible light. *J. Colloid Interface Sci.* **2000**, *224*, 202-204.
28. Zhu, J.; Chen, F.; Zhang, J.; Chen, H.; Anpo, M. Fe⁺³-TiO₂ Photocatalysts prepared by combining sol – gel method with hydrothermal treatment and their characterization. *J. Photochem. Photobiol. A* **2006**, *180*, 196-204.
29. Likodimos, V.; Stergiopoulos, T.; Falaras, P.; Kunze, J.; Schmuki, P. Phase composition, size, orientation, and antenna effects of self assembled anodized titania nanotube arrays: A polarized micro raman investigation. *J. Phys. Chem. C* **2008**, *112*, 12687-12696.
30. Chen, X.; Liu, L.; Yu, P.Y.; Mao, S.S. Increasing solar absorption for photocatalysis with black hydrogenated titanium dioxide nanocrystals. *Science* **2011**, *331*, 746-750.
31. Brahim, R.; Bessekhoud, Y.; Bouguelia, A.; Tarari, M. Visible light induced hydrogen evolution over the heterosystem Bi₂S₃/TiO₂. *Catal. Today* **2007**, *122*, 62-65.
32. Ghows, N.; Entezari M.H. Fast and easy synthesis of core shell nanocrystal CdS/TiO₂ at low temperature by micro emulsion under ultrasound. *Ultrason. Sonochem.* **2011**, *18*, 629-634.